Nonlocal vortex motion in mesoscopic amorphous Nb0.7Ge0.3 structures

Helzel, A.; Kokanović, Ivan; Babić, Dinko; Litvin, L. V.; Rohlfing, F.; Otto, F.; Surgers, C.; Strunk, C.

Source / Izvornik: **Physical review B: Condensed matter and materials physics, 2006, 74**

Journal article, Published version
Rad u časopisu, Objavljena verzija rada (izdavačev PDF)

https://doi.org/10.1103/PhysRevB.74.220510

Permanent link / Trajna poveznica: https://urn.nsk.hr/urn:nbn:hr:217:995955

PHYSICAL REVIEW B **74**, 220510(R) (2006)

Nonlocal vortex motion in mesoscopic amorphous $Nb_{0.7}Ge_{0.3}$ structures

A. Helzel,[1] I. Kokanović,[1,2] D. Babić,[2,*] L. V. Litvin,[1] F. Rohlfing,[1] F. Otto,[1] C. Sürgers,[3] and C. Strunk[1]
[1]*Institute for Experimental and Applied Physics, University of Regensburg, D-93025 Regensburg, Germany*
[2]*Department of Physics, Faculty of Science, University of Zagreb, Bijenička 32, HR-10000 Zagreb, Croatia*
[3]*Physikalisches Institut and DFG Center for Functional Nanostructures (CFN), Universität Karlsruhe, D-76128 Karlsruhe, Germany*
(Received 16 June 2006; revised manuscript received 20 September 2006; published 18 December 2006)

We study nonlocal vortex transport in mesoscopic amorphous $Nb_{0.7}Ge_{0.3}$ samples. A dc current I is passed through a wire connected via a perpendicular channel, of a length $L=2-5$ μm, with a pair of voltage probes where a nonlocal response $V_{nl} \propto I$ is measured. The maximum of $R_{nl}=V_{nl}/I$ for a given temperature occurs at an L-independent magnetic field and is proportional to $1/L$. The results are interpreted in terms of the dissipative vortex motion along the channel driven by a remote current and can be understood in terms of a simple model.

DOI: 10.1103/PhysRevB.74.220510 PACS number(s): 74.78.Na, 74.78.Db, 74.25.Qt, 74.25.Fy

In a pioneering work Giaver measured a magnetic-flux-transformer effect in type-II superconductors.[1] He applied a magnetic field B perpendicularly to a sample comprising two superconducting sheets separated by a thin insulator, passed a current I through one of the superconductors, and measured a voltage developed over the other one—where no current was flowing. The induced voltage was a consequence of an electromagnetic coupling of vortices in the two layers. In their recent experiment Grigorieva *et al.*[2] demonstrated a complementary flux-transformer phenomenon associated with vortices. They produced mesoscopic amorphous MoGe structures of a double-cross shape, consisting of two parallel wires connected at a right angle by a channel of width $w=0.07-2$ μm and a length $L=0.5-12$ μm. In a perpendicular B and with I through one of the parallel wires a nonlocal voltage V_{nl} appeared over the second, current-free wire. This novel, transversal flux-transformer effect originated in the in-plane vortex-vortex repulsion, which conveyed the driving force from the current-carrying wire to the vortices in the channel. The effect disappeared not only for L exceeding $6-7$ μm but also for w larger than $\sim 0.5-1$ μm. When w was sufficiently small the force on the vortices in the channel was transferred over many intervortex distances and, moreover, V_{nl} was proportional to I. The efficiency of the transversal flux-transformer effect can be quantified by a nonlocal resistance $R_{nl}=V_{nl}/I$.

In the experiment of Grigorieva *et al.*[2] the local mixed-state dissipation was characterized on separate mm-sized films, whereas V_{nl} was measured by a low-frequency ac method during B sweeps at constant temperatures T. An ac method was used because V_{nl} was in nV range—i.e., $R_{nl}<5$ mΩ—thus being too small for dc detection. In our work we focused on dc probing of the transversal flux-transformer effect and measuring V_{nl} and the local voltage V_l on the same sample, which was possible in multiterminal amorphous $(a-)Nb_{0.7}Ge_{0.3}$ structures of the geometry shown in the inset to Fig. 1. The weak pinning, characteristic of the $a-Nb_{0.7}Ge_{0.3}$ material used, resulted in a dc-measurable V_{nl} and $R_{nl} \sim 1$ Ω even at very low temperatures. The measured nonlocal resistance was hence two orders of magnitude larger than in Ref. 2.

In this study we investigate the transversal flux-transformer effect in samples of different length by isothermal sweeps of B, over a range of applied I and for $0.15T_c \lesssim T \lesssim 0.95T_c$, where T_c is the superconducting transition temperature. V_{nl} depends linearly on I in the range $I=0.1-1$ μA. With increasing B, $R_{nl}(B)$ first acquires a nonzero value at $B=B_d$, then has a maximum at $B=B_p$, and gradually vanishes close to the upper critical magnetic field B_{c2}. The main representatives of R_{nl}—i.e., B_p and $R_p=R_{nl}(B_p)$—behave differently with respect to the channel length. B_p is independent of L whereas $R_p \propto 1/L$, suggesting a vortex velocity $u_{nl} \propto 1/L$ at the nonlocal voltage probes. This we relate to the total frictional force on the vortices in the channel being proportional to L.

We investigated two structures of the type shown in the inset to Fig. 1, where we also assign numbers to the leads and define the coordinate system (with the unit vectors $\hat{\mathbf{x}}$, $\hat{\mathbf{y}}$ and $\hat{\mathbf{z}}$). As in our previous studies,[3,4] the samples were produced by combining electron-beam lithography with magnetron sputtering but the film thickness was increased from 20 nm to $d=60$ nm in order to safely avoid inhomogeneities detected in samples of a cross section smaller than

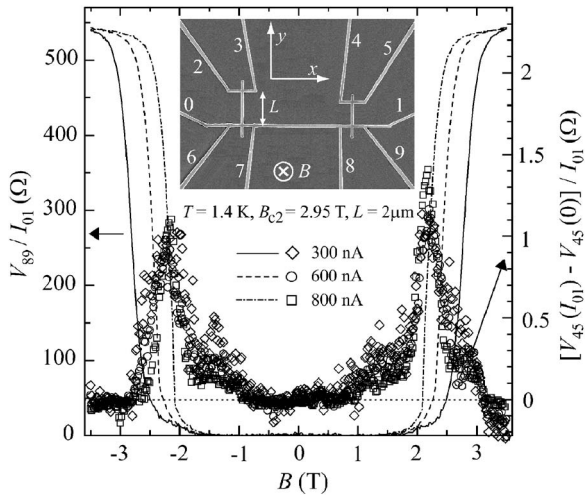

FIG. 1. Local (lines, left-hand scale) and nonlocal (symbols, right-hand scale) response for the $L=2$ μm channel at $T=1.4$ K ($B_{c2}=2.95$ T) and $I=I_{01}=300, 600, 800$ nA. Inset: a photograph of the sample, with the designation of the leads and the definition of the coordinate system.

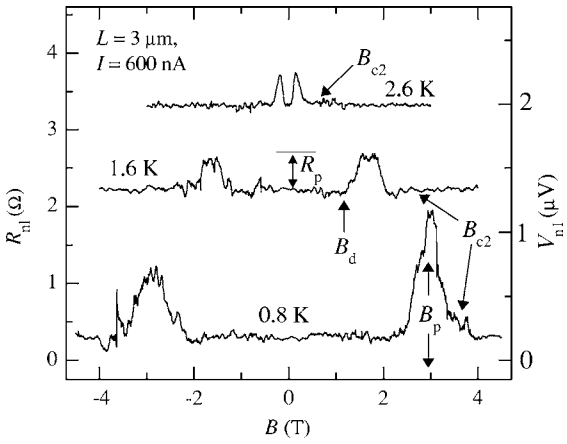

FIG. 2. $R_{nl}(B)$ (left-hand scale) for an $L=3$ μm channel at $T=0.8, 1.6, 2.6$ K and $I=600$ nA, with the voltage resolution shown by the right-hand scale. The curves are offset for clarity. The meaning of B_d, B_p, and R_p is indicated by the arrows.

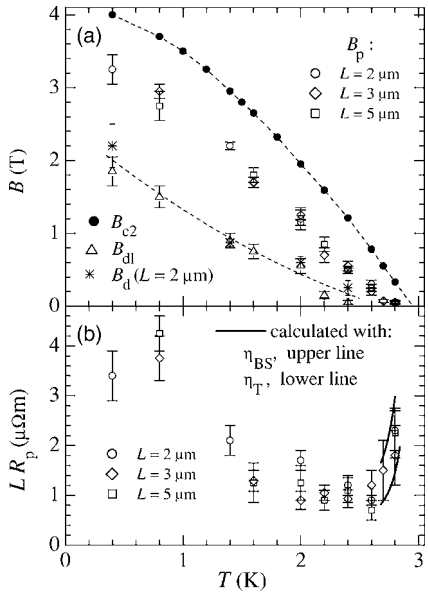

FIG. 3. Characteristic parameters of R_{nl} for the three channel lengths. (a) $B_p(T)$ together with $B_{c2}(T)$, $B_{dl}(T)$, and $B_d(T)$ for the $L=2$ μm channel. The dashed lines are guides for the eye. (b) LR_p vs T. The solid lines represent the results of the calculations (using η_{BS} and η_T, as indicated) explained in the text.

~ 5000 nm^2. This way the pinning was enhanced, as we inferred from the local dissipation, but still remained weak enough to permit a nonlocal vortex motion over several microns. Contacts 0 and 1 are used for applying a dc $I=I_{01}$ through the horizontal wire, exerting a local force on vortices in the y direction (since $\mathbf{B}=-B\hat{\mathbf{z}}$). Having a velocity $\mathbf{u}=u\hat{\mathbf{y}}$, vortices induce an electric field $\mathbf{E}=E\hat{\mathbf{x}}$. Combinations of contacts $i,j=6-9$ are used for measuring the local voltage drop V_l. The local vortex pressure is transferred from the horizontal wire along the zero-I channels (the length L is indicated for the left channel) toward the crosses contacted by leads 2,3 and 4,5, where V_{nl} is measured. For the first sample the channel lengths were 2 and 3 μm and for the second 3 and 5 μm, so we covered the range $L=2-5$ μm and had two $L=3$ μm samples for a consistency check. All wires of a single sample had the same width: $w=275$ nm for the sample with the longer channels and $w=250$ nm for the other one. This small difference did not affect the results presented henceforth. Since dc measurements are invariably burdened by sub-μV parasitic signals, in order to determine $V_{nl}(I)$ for a given measurement with leads i, j we recorded both $V_{nl,ij}(I)$ and $V_{nl,ij}(I=0)$ taken at the same B-sweep rate and direction. $V_{nl,ij}(I=0)$ was different for different pairs of leads and depended very weakly on the B-sweep rate. The background-free nonlocal voltage was extracted as $V_{nl}(I)=V_{nl,ij}(I)-V_{nl,ij}(I=0)$. By this procedure we found a very regular behavior of $V_{nl}(I)$, which, in particular, for the two $L=3$ μm channels agreed within the error bars. From the local voltage response between contacts (8,9) we characterized the samples in the same way as in our previous work,[3] obtaining $T_c=2.95$ K, the normal-state resistivity $\rho_n=3.7$ $\mu\Omega$ m, $-(dB_{c2}/dT)_{T=T_c}=2.17$ T/K, and the Ginzburg-Landau parameters $\kappa=100$, $\xi(0)=7.15$ nm, and $\lambda(0)=1.18$ μm.

Results typical of *Vnl* are shown in Figs. 1 and 2. The data in Fig. 1 were obtained for the $L=2$ μm channel at $T=1.4$ K ($B_{c2}=2.95$ T) and with $I=I_{01}=300, 600, 800$ nA. The lines (left-hand scale) correspond to the local response V_{89}/I_{01}, and the symbols (right-hand scale) to $V_{nl}/I=[V_{45}(I_{01})-V_{45}(0)]/I_{01}$. As expected from previous investigations[3] of $V(I)$ of $a-Nb_{0.7}Ge_{0.3}$, for the given current density $J\sim 20-50$ MA/m^2 the local response at low T depends on I. Noteworthy, in contrast to $d=20$ nm samples with a weaker pinning[3,4] the onset of V_l at a certain $B=B_{dl}$ is essentially independent of I. B_{dl} nearly coincides with B_d for $L=2$ μm, while B_d for $L=3$, 5 μm is higher for $\sim 5\%$ (high T) to $\sim 20\%$ (low T) and mutually indistinguishable. Contrary to $V_l(I)$, $V_{nl}(I)$ is for the given range of I linear for all T.[5]

In Fig. 2 we show how $R_{nl}=V_{nl}/I$ changes with temperature. The results refer to an $L=3$ μm channel, $I=600$ nA, and $T=0.8, 1.6, 2.6$ K. As in Fig. 1, $R_{nl}=0$ up to $B=B_d$ after which it displays a relatively broad peak around $B=B_p$, which defines $R_p=R_{nl}(B_p)$. Close to the B_{c2}, R_{nl} drops to zero again. While the nonlocal resistance in Ref. 2 decreased with decreasing T, vanishing at $T/T_c\sim 0.6$, in our experiment we find a nonmonotonic variation of $R_{nl}(T)$. R_{nl} is finite even at the lowest measurement temperature ($T=0.4$ K, $T/T_c\approx 0.14$), decreases at low T, and increases close to T_c with increasing T [see Fig. 3(b) later]. The $R_{nl}(B)$ traces are nearly symmetric around $B=0$, but especially at low T and/or high I, R_p for $B<0$ and $B>0$ may differ to some extent, as seen, e.g., in Fig. 1 for $I=800$ nA (1.4 K) and in Fig. 2 for $T=0.8$ K (600 nA). These differences do not necessarily appear only because of variations in measurement conditions during the long B sweeps (e.g., slightly different bath temperature); they may also originate in the Nernst effect[6] due to a heating in the current-carrying wire.[3] However, the Nernst effect changes sign by reversal of B and can be canceled by the averaging $R_{nl}(B)=[R_{nl}(+B)+R_{nl}(-B)]/2$. Moreover, for our samples $R_{nl}(+I)=R_{nl}(-I)$, which rules out a rectifying effect proposed recently.[7]

Essential information on R_{nl} is contained in the characteristic quantities B_p and R_p. In Fig. 3(a) we plot $B_p(T)$ for all three channel lengths, together with $B_{c2}(T)$, $B_{dl}(T)$, and $B_d(T)$ for the $L=2$ μm channel. B_{dl} and B_d are relatively low and become immeasurably small above 2.6 K (this applies to B_d for $L=3$, 5 μm as well). It can be seen that B_p is independent of L. On the other hand, R_p does depend on L, which is shown in Fig. 3(b). R_pL vs T, plotted by the symbols, exhibits a reasonably well-defined scaling behavior, implying $R_p \propto 1/L$.

Before turning to a more quantitative description of the data we would like to give an intuitive picture of the nonlocal effects observed. As discussed in Ref. 2, J decays with distance y from the local cross as $\propto \exp(-\pi y/w)$. Hence, for the range of L in our experiment the weak penetration of J into the channel is of little importance. For magnetic fields $B<B_{dl}$ both V_l and V_{nl} must be zero since vortices do not move at all due to the pinning. On the other hand, for $B>B_{c2}$ the vortex contribution to V_{nl} must vanish, since the sample is normal. A more intricate question is the relation between the local dynamics where $J\neq 0$ and the nonlocal vortex motion where $J=0$, especially because vortex transport in the presence of pinning (i.e., at low T) depends strongly on J. The direct comparison of V_l and V_{nl} is complicated further by the different conditions for vortex motion in the local cross (vortices face other vortices in the channel) and in the rest of the local wire (vortices face either surface barriers, if present, or vacuum at the edges). However, in spite of these difficulties the presented results can be explained reasonably well by a simple model discussed below, which agrees with the data even quantitatively when the pinning is negligible.

This model assumes equilibrium between the driving force exerted by I on the vortices in the lower cross and the frictional damping force on the vortices in the channel, as well as the presence of surface barriers enforcing a dominating y component of u inside the channel. In a first step we neglect the pinning and assume that the frictional force is linear in u with a velocity-independent friction coefficient η. The effects of pinning are addressed later.

At a vortex density $n_\phi=B/\phi_0$, where ϕ_0 is the magnetic-flux quantum, in total $n_\phi w^2$ vortices in the lower cross—each experiencing a force $J\phi_0 d$—apply a pressure $p=n_\phi\phi_0 I/d$ on the vortices in the channel. The corresponding pushing force (per unit vortex length) pw is balanced by the force required to move $n_\phi Lw$ vortices along the channel against the frictional damping ηu_{nl} per vortex. This gives $u_{nl}=\phi_0 I/\eta Ld \propto 1/L$. Using $V_{nl}=wBu_{nl}$ we find

$$R_{nl}=\frac{V_{nl}}{I}=\frac{\phi_0 Bw}{L\eta d}. \quad (1)$$

The above result holds if the surface barriers are strong enough to confine the vortex motion within the channel. As shown experimentally in Ref. 2, this is not satisfied for large w. In any case, surface barriers are essential to preserve the uniaxial character of the nonlocal vortex motion. An important source of the surface barriers is the Meissner currents J_M flowing along the channel edges and providing an inward-pointing force $F_{in}\propto J_M$. The surface barriers weaken by approaching B_{c2} irrespective of their exact origin, which may explain the fact that $R_{nl}(B)$ does not increase all the way up to $B=B_{c2}$ before dropping to zero in the normal state. This restricts the range of applicability of Eq. (1) to B not too close to B_{c2}. On the other hand, Eq. (1) correctly reproduces[8] $R_p\propto 1/L$ and, as we show below, accounts for $R_p(T)$ quantitatively in conditions of insignificant pinning.

For $T\geqslant 2.7$ K the $V_l(I)$ curves are linear beyond any doubt, implying a negligible pinning and, moreover, $\eta\approx\eta_f$ of the viscous drag in pure flux flow. There are two possible dissipation mechanisms that determine the flux-flow viscosity η_f.[9] One is related to Joule heating of normal electrons in vortex cores by the E therein, as described by the Bardeen-Stephen model giving $\eta_f=\eta_{BS}=\phi_0 B_{c2}/\rho_n$.[10] The other approach, proposed by Tinkham, attributes the dissipation to a loss of the superconducting Gibbs free-energy density $G_s(B,T)$ as vortices move and cause depairing and recombination of Cooper pairs.[11] This process is affected by the time $\tau=(\hbar/\Delta_0)[1+(T/T_c)^2]/[1-(T/T_c)^2]$ of establishing a superconducting state and results in $\eta_f=\eta_T=2\pi\tau G_s$ ($\Delta_0\approx 1.76k_BT_c$ is the superconducting gap at $T=0$ and $\hbar$ the Planck constant).[11] For B not too close to B_{c2}—i.e., in the regime of the applicability of Eq. (1)—G_s can be approximated by the superconducting condensation energy $U_s(T)\approx B_{c2}^2(T)/4\kappa^2\mu_0$, where $\mu_0=4\pi/10^7$ H/m.[3] Since we know $B_{c2}(T)$, we can determine both η_{BS} and η_T for our samples, which permits a quantitative comparison of the experiment and the model.

At $T\gtrsim 2.7$ K the measured $B_p\approx 60$ mT$\ll B_{c2}$ is fairly constant, so the temperature dependence of the corresponding R_p is dominated by that of η. By calculating η_{BS} and η_T without any adjustable parameter and using Eq. (1) we obtain LR_p shown in Fig. 3(b) by the solid lines, as indicated. The magnitudes of measured and calculated R_p agree well, and this result is only weakly sensitive to precise T dependences of B_p and η. It is suggestive that, although restricted to a narrow T range of negligible pinning, our model can also reproduce the steep increase of $R_p(T)$ near T_c, which is attributed to a rapid decay of η_f preceding the transition to the normal state and vanishing of R_{nl}.

So far we have not included any effect of pinning into our analysis, which is justified only in a narrow T range close to T_c. At lower temperatures the use of η_f and the measured values of B_p in Eq. (1) results in a rapid increase of R_p far above the observed values. In addition, nonlinearities in $V_l(I)$ are observed below 2.7 K, indicating that the pinning is no longer marginal. However, the fact that the linearity of $V_{nl}(I)$ and $R_p\propto 1/L$ are preserved in this regime brings up a possibility of extending our model to lower temperatures. This is achievable if even in the presence of pinning p remains proportional to I and η independent of u. Below we argue that these properties are consistent with a plausible picture of the distribution of the pinning force in our samples.

We recall that the onset of V_l at B_{dl} does not depend on I, which suggests a critical vortex density for triggering the dissipation. This implies that for $B<B_{dl}$ the flux is first trapped in the most-strong-pinning regions of the sample.[12] When these are saturated at $B=B_{dl}$ vortices enter the lower-

pinning regions in between—where they can move more easily. Only after this saturation does the dissipation start by the vortex motion along "vortex rivers" between the strong-pinning sites and areas. In the current-carrying wire vortices in the "rivers" shear plastically with the edges, thus enhancing the driving force above $J\phi_0$ in depinning the vortices. This process may result in a nonlinear $V_l(I)$, such as that observed in Fig. 1, because one such vortex driven constantly by J assists in depinning several vortices close to its path through a "river." Since J supplies energy for the depinning described, the nonlinearity cannot propagate significantly into the channel where $J \propto \exp(-\pi y/w)$.[2] The pushing force is thus conveyed along the "rivers" set by the equilibrium pinning properties, and the fraction of the contributing vortices is $f \sim (B-B_{dl})/B$. The vortex pressure is therefore reduced by the same factor f.

The frictional damping of the vortex motion in "vortex rivers" was investigated in samples with artificial easy-flow channels embedded in a strong-pinning medium.[13] Because of the random pinning landscape in our samples, no commensurability effects between the moving and immobile vortex regions are expected and the vortex velocity in the "rivers" should respond linearly to the applied force. This may explain the observed linearity of $V_{nl}(I)$, while the magnitude of R_{nl} is reduced by the ratio f that accounts for the number of vortices in the strong-pinning regions. Although we lack a manageable model for calculating η including the effects of pinning, the increase of R_p as T is lowered can be explained at least qualitatively as a consequence of $B_p(T)$ growing faster than $\eta(T)$.

To conclude, we have investigated a transversal flux-transformer effect, manifested in a nonlocal flow of vortices in a narrow superconducting channel driven by a remote dc current. In our low-pinning a-$Nb_{0.7}Ge_{0.3}$ the nonlocal voltage appears in more than half of the superconducting phase diagram—i.e., everywhere where the vortices can be moved easily enough to induce dissipation at very low currents. The effect is two orders of magnitude larger than in previous studies.[2] We observe a nonmonotonic variation of the maximal nonlocal resistance with temperature, which can be explained by an interplay of vortex density and vortex-motion viscosity. Close to T_c the data are in quantitative agreement with a simple model based on the assumption that the vortices behave like a weakly compressible fluid confined to the superconducting channel by surface barriers.

We thank E. H. Brandt and C. Morais Smith for helpful discussions. This work has been financially supported by the DFG within GRK 638 and SFB 631 and by the Croatian MZOS under Project No. 119262.

*Corresponding author. Electronic address: dbabic@phy.hr

[1] I. Giaver, Phys. Rev. Lett. **15**, 825 (1965).
[2] I. V. Grigorieva *et al.*, Phys. Rev. Lett. **92**, 237001 (2004).
[3] D. Babić *et al.*, Phys. Rev. B **69**, 092510 (2004), and references therein.
[4] J. Bentner *et al.*, Phys. Rev. B **70**, 184516 (2004).
[5] A significant decay of R_{nl} appears around $I=1.2$ μA.
[6] M. Zeh *et al.*, Phys. Rev. Lett. **64**, 3195 (1990).
[7] D. Y. Vodolazov *et al.*, Phys. Rev. B **72**, 024537 (2005).
[8] The 1-μm-long tails of the crosses, outside the channel area, do not add to the damping force. F_{in} pushes vortices inwards along the y direction as well, so the contributions of the tails cancel out and L is the proper length for the vortex-block size.
[9] A. I. Larkin and Yu. N. Ovchinnikov, in *Nonequilibrium Superconductivity*, edited by D. N. Langenberg and A. I. Larkin (North Holland, Amsterdam, 1986).
[10] J. Bardeen and M. J. Stephen, Phys. Rev. **140**, A1197 (1965).
[11] M. Tinkham, Phys. Rev. Lett. **13**, 804 (1964).
[12] T. Matsuda *et al.*, Science **271**, 1394 (1996).
[13] T. Dröse *et al.*, Phys. Rev. B **67**, 064508 (2003).